

Phase diagram of compact QED coupled to a four-Fermi interaction

John B. Kogut

Physics Department, University of Illinois at Urbana-Champaign, Urbana, Illinois 61801-3080

Costas G. Strouthos

Department of Physics, University of Wales Swansea, Singleton Park, Swansea, SA2 8PP, United Kingdom

(Received 12 November 2002; published 19 February 2003)

Compact lattice quantum electrodynamics with four species of fermions is simulated with massless quarks by adding a four-Fermi interaction to the action. Simulations in the chiral limit are done on 8^4 lattices for exploratory purposes, and 16^4 lattices for quantitative purposes, and the phase diagram, parametrized by the gauge and the four-Fermi couplings, is mapped out. The line of monopole condensation transitions is separate from the line of chiral symmetry restoration as long as the four-Fermi coupling is not too small. The simulation results indicate that the monopole condensation transition is first order while the chiral transition is second order. The challenges in determining the universality class of the chiral transition are discussed. If the scaling region for the chiral transition is sufficiently wide, the 16^4 simulations predict critical indices far from mean field values. We briefly discuss a speculative scenario in which antiscreening provided by strands of bound monopole and antimonopole loops is the agent that balances the screening of fermion-antifermion pairs to produce ultraviolet stable fixed points.

DOI: 10.1103/PhysRevD.67.034504

PACS number(s): 11.15.Ha

I. INTRODUCTION

The coupled system of four-Fermi interactions and Abelian gauge fields has been of interest to model builders, phenomenologists, and theorists for some time. In the context of noncompact lattice QED, this approach has been used to show the logarithmic triviality of noncompact QED with dynamical fermions [1].

In this paper we study the compact version of the model. We are particularly interested in the chiral transition and its scaling properties as well as the model's magnetic monopoles and their possible effect on the continuum limit of the chiral transition. The compact version of QED with dynamical fermions has not been studied as well as the noncompact version of the model. The model will be simulated using the hybrid molecular dynamics (HMD) algorithm [2].

The compact version of four-flavor QED has interactions coming from photons and magnetic monopoles coded into the compact gauge fields. By adding a four-Fermi interaction which preserves a piece of the chiral symmetry of the massless model, we can study light fermions directly on the lattice and see how fermion charge screening affects the dynamics. The four-Fermi interaction also gives us the opportunity to separate the chiral transition of the model from its confinement or deconfinement transition which is controlled by monopole condensation.

It is crucial in all of this that fermion screening be accounted for accurately and realistically. It is inappropriate to make any simplifications here because the character of fermion screening is not understood outside perturbation theory. Some unbiased simulation studies are called for to see if, for example, the antiscreening due to magnetic monopoles can balance the screening due to fermion loops and lead to ultraviolet stable fixed points [3]. This need further motivates us to consider the version of the model with an explicit four-Fermi interaction because then no bare fermion mass is

needed to ensure convergence of the algorithm [4] and we are guaranteed that the fermions remain light even on the strongly cutoff lattice.

Our lattice model has two couplings: the conventional gauge coupling of compact QED and the four-Fermi coupling of the Nambu–Jona-Lasinio term. The uncoupled versions of compact QED and the Nambu–Jona-Lasinio models have been studied by lattice gauge theory methods and considerable quantitative information is available to guide this study. We shall find two lines of transitions in the two-dimensional coupling constant parameter space of the compact QED-gauged Nambu–Jona-Lasinio model. One line is associated with monopole condensation and the other with chiral symmetry breaking. Long runs on fairly large lattices, 16^4 , indicate that the monopole condensation transition is first order. A finite size scaling analysis of this transition is necessary to state this result with “absolute” certainty and such a study must await more computer resources. Simulations on 24^4 and 32^4 are in the planning stages. However, much more intensive recent studies which determined the scaling behavior of the latent heat [5] have produced quite decisive evidence for the first order character of this transition in the theory without fermions. Although our major concern here focuses on the chiral transition, which has not been studied quantitatively before, it is a good test of our methods and statistics that our data on the confinement-deconfinement transition are very abrupt and favor first order.

The line of chiral transitions is distinct from the line of monopole transitions as long as the four-Fermi term is not too small. One point along the line of chiral transitions is studied in detail to determine the character of the chiral transition. This work parallels recent studies of the noncompact version of the model which concluded that the chiral transition was logarithmically trivial [1]. Conventional “wisdom” would suggest the same result here, since the monopole concentration vanishes on the line of chiral transitions. However,

this result is far from clear in our numerical work. The best fits to the chiral condensate and its associated susceptibility are compatible with power laws of a second order transition, but the critical indices are far from the expected mean field values. Unfortunately, the immediate vicinity of the critical point cannot be well studied on this size lattice, 16^4 , because of finite size effects, so the simulations reported here might not be registering the real continuum scaling laws of the theory. Simulations on larger lattices closer to the critical point are required and studies on 24^4 and 32^4 lattices are planned.

This paper is organized as follows. In the next section we present the formulation of the lattice action and discuss its symmetries and general features. In the third section we sketch the phase diagram and in the fourth section, the heart of the paper, we examine several points in the phase diagram in detail and come to preliminary quantitative conclusions about the first order character of the monopole condensation transition and the second order character of the chiral transition. In the fifth section we comment on the puzzling nature of the results, briefly present a physical picture of a non-trivial chiral transition in which antiscreening due to entwined loops of magnetic monopoles and antimonopoles balances screening due to fermion-antifermion pairs, and suggest further research.

II. FORMULATION

To begin, consider the Abelian-gauged Nambu–Jona-Lasinio model with four species of fermions. The Lagrangian for the continuum gauged Nambu–Jona-Lasinio model is

$$L = \bar{\psi}(i\gamma\partial - e\gamma A - m)\psi - \frac{1}{2}G(\bar{\psi}\psi)^2 - \frac{1}{4}F^2. \quad (1)$$

The Lagrangian has an electromagnetic interaction with continuous chiral invariance ($\psi \rightarrow e^{i\alpha\tau\gamma_5}\psi$, where τ is the appropriate flavor matrix) and a four-Fermi interaction with discrete (Z_2) chiral invariance ($\psi \rightarrow \gamma_5\psi$). The mass term $m\bar{\psi}\psi$ breaks the chiral symmetries and will be set to zero in much of the work that follows. The pure Nambu–Jona-Lasinio model has been solved at large N by gap equation methods [6], and an accurate simulation study of it has been presented [4]. The discrete (Z_2) chiral invariant action produces a particularly efficient algorithm. Full chiral symmetry should be restored naturally in the continuum limit in those regions of the parameter space where the four-Fermi term proves to be irrelevant. The action with Z_2 chiral symmetry is preferable for simulation studies over models with continuous chiral symmetry because the latter are not as efficiently simulated due to massless modes in the strongly cut-off theory.

It is useful to introduce an auxiliary random field σ by adding $-(G/2)[(\bar{\psi}\psi) - \sigma/G]^2$ to the Lagrangian. This makes the Lagrangian a quadratic form in the fermion field so it can be analyzed and simulated by conventional methods. The model is then discretized by using staggered fermions.

The lattice action reads, in the case where the gauge symmetry is interpreted as a compact local $U(1)$ symmetry, following Wilson’s original proposal [7],

$$S = \sum_{x,y} \bar{\psi}(x)(M_{xy} + D_{xy})\psi(y) + \frac{1}{2G} \sum_{\tilde{x}} \sigma^2(\tilde{x}) + \frac{1}{2e^2} \sum_{x,\mu,\nu} \{1 - \cos[F_{\mu\nu}(x)]\} \quad (2)$$

where

$$F_{\mu\nu}(x) = \theta_\mu(x) + \theta_\nu(x + \hat{\mu}) + \theta_{-\mu}(x + \hat{\mu} + \hat{\nu}) + \theta_{-\nu}(x + \hat{\nu}), \quad (3)$$

$$M_{xy} = \left(m + \frac{1}{16} \sum_{\langle x, \tilde{x} \rangle} \sigma(\tilde{x}) \right) \delta_{xy}, \quad (4)$$

$$D_{xy} = \frac{1}{2} \sum_{\mu} \eta_\mu(x) (e^{i\theta_\mu(x)} \delta_{x+\hat{\mu},y} - e^{-i\theta_\mu(y)} \delta_{x-\hat{\mu},y}), \quad (5)$$

where σ is an auxiliary scalar field defined on the sites of the dual lattice \tilde{x} [8], and the symbol $\langle x, \tilde{x} \rangle$ denotes the set of the 16 lattice sites surrounding the direct site x . The factors $e^{\pm i\theta_\mu}$ are the gauge connections and $\eta_\mu(x)$ are the staggered phases, the lattice analogues of the Dirac matrices. ψ is a staggered fermion field and m is the bare fermion mass, which will be set to 0. Note that the lattice expression for $F_{\mu\nu}$ is the circulation of the lattice field θ_μ around a closed plaquette, the gauge field couples to the fermion field through compact phase factors to guarantee local gauge invariance, and $\cos F_{\mu\nu}$ enters the action to make it compact.

It will often prove convenient to parametrize results with the inverse of the four-Fermi coupling, $\lambda \equiv 1/G$, and the inverse of the square of the gauge coupling, $\beta \equiv 1/e^2$.

The global discrete chiral symmetry of the action reads

$$\psi(x) \rightarrow (-1)^{x_1+x_2+x_3+x_4} \psi(x), \quad (6)$$

$$\bar{\psi}(x) \rightarrow -\bar{\psi}(x) (-1)^{x_1+x_2+x_3+x_4}, \quad (7)$$

$$\sigma \rightarrow -\sigma, \quad (8)$$

where $(-1)^{x_1+x_2+x_3+x_4}$ is the lattice representation of γ_5 .

As we mentioned, interesting limiting cases of the above action are (1) the Z_2 Nambu–Jona-Lasinio model with no gauge fields, which has a chiral phase transition at $G \approx 2.0(1)$ [4]; (2) the compact QED model with no four-Fermi interactions, whose first order chiral phase transition is coincident with its first order monopole condensation transition near $\beta \equiv 1/e^2 \approx 0.89(1)$ for four flavors [9]; and (3) the $G \rightarrow \infty$ case in which the fermions obtain a dynamical mass comparable to the reciprocal of the lattice spacing and therefore decouple, leaving quenched compact QED which has a first order transition at $\beta = 1.011124(1)$ [5].

The lattice simulation code is very similar to others in this program. The systematic step size errors, those varying as dt^2 , the discretization of the molecular dynamics evolution equations in HMD “time” t , have been studied in the past

and are understood [4,1]. Taking $dt \leq 0.01$ produced chiral condensates whose systematic errors were considerably smaller than their statistical errors. Other algorithmic problems, such as finite size effects, tunnelling, and long correlation times were monitored carefully in the runs and will be discussed below when appropriate.

III. PHASE DIAGRAM

Our first task was to map out the two-dimensional parameter space (β, G) using the hybrid molecular dynamics algorithm tuned for four continuum fermion species [2]. We measured the chiral condensate and its susceptibility and the monopole concentration and its susceptibility as a function of β and G on an 8^4 lattice. These observables have been discussed extensively in the literature and we refer the reader to [9,10] for background. The expectation value of the field σ is proportional to $\bar{\psi}\psi$ in these models and serves as its chiral order parameter.

The 8^4 simulations were done simply to explore the phase diagram and prepare for the more quantitative 16^4 simulations that will be analyzed below. We know from past related studies [4] that 8^4 lattices are not large enough for finite size scaling analyses or other quantitative purposes, so these runs will not be presented in detail.

For very small G the chiral transition and the monopole condensation transition were coincident to the accuracy and resolution of our survey. Abrupt jumps in the order parameters were measured and were interpreted as signalling first order transitions. Earlier studies of compact QED with no four-Fermi interactions [9] presented evidence for first order coincident chiral and monopole condensation transitions in good agreement with this study.

As G was increased from zero, we found that the line of chiral transitions and the line of monopole condensation transitions become clearly distinct. We will show measurements at fixed $\lambda = 1/G = 1.40$ and variable β on a 16^4 lattice which will make this point very clear. In particular, setting $\lambda = 1/G = 1.40$ and then increasing β in small steps from the strong coupling region of $\beta \ll 1.0$, we shall see good evidence for an abrupt transition in the monopole concentration M at $\beta \approx 0.95$. M is large, approximately 0.87, at $\beta = 0.953125$ and $\lambda = 1.40$, while it is small, approximately 0.018, at $\beta = 0.9625$ and $\lambda = 1.40$. Throughout this region of the phase diagram, the chiral condensate σ is distinctly non-zero, so the system resides in the chirally broken phase even though M vanishes. The chiral order parameter σ does, however, experience a jump from $\sigma \approx 0.55$ at $\beta = 0.953125$ and $\lambda = 1.40$ to $\sigma \approx 0.44$ at $\beta = 0.9625$ and $\lambda = 1.40$, indicating that free monopoles do contribute to chiral symmetry breaking, as expected, but the gauge coupling is sufficiently large in this case that chiral symmetry breaking occurs even without the active participation of free monopoles. In fact, as β increases further at fixed $\lambda = 1.40$, σ falls slowly and it is not until $\beta \approx 1.393$ that it vanishes. The vanishing appears to be continuous. The chiral transition will be discussed in more detail below. However, it was easy to determine that the chiral transition occurs at a smaller gauge coupling e^2 at fixed $\lambda = 1.40$ than the confinement-deconfinement transi-

tion, and the two transitions, whatever their orders, are separate and distinct.

The line of chiral symmetry breaking transitions continues to larger G and higher β from the point $\lambda = 1/G = 1.40$ and $\beta = 1.393$ studied carefully here. We know from previous work [4] that the four-Fermi coupling alone breaks chiral symmetry at strong coupling, $G \approx 2.0$. Those studies of the four-Fermi model were done with care and the logarithmic triviality of the Nambu–Jona-Lasinio model was confirmed. This established that the four-Fermi interaction is indeed irrelevant if gauge fields are absent.

The first order line of monopole condensation transitions extends to higher G from the point $\lambda = 1/G = 1.40$ and $\beta = 0.956$ emphasized here. In fact it moves to only slightly weaker coupling e as G grows large. We will study it carefully by simulating the two-coupling model at fixed $\beta = 1.0$ and variable G and find evidence for a first order monopole condensation point at $\beta = 1.0$ and $G \approx 1.8$ where M jumps discontinuously from zero to a large value. We will see that σ is large and stable in the vicinity of this monopole condensation point, on both sides of it. Therefore, the fermions have an effective mass comparable to the cutoff energy and should decouple from continuum physics, if there is any, in the model. In any case, the model should not be significantly different from compact QED without fermions and its monopole condensation should be essentially the same as in the model with only gauge fields. We support the view that the monopole condensation transition, which also signals the confinement-deconfinement transition in the gauge theory without fermions, is first order. Recent simulations of compact QED without fermions, which do careful finite size scaling studies, have provided quantitative, convincing evidence for this result [5].

IV. 16^4 SIMULATIONS AT FIXED $\lambda = 1.4$

Consider the observables, the chiral condensate and its susceptibility and the monopole concentration and its susceptibility, as recorded in Table I. In this case the strength of the four-Fermi interaction is set to a constant $\lambda = 1.4$ and the gauge coupling varies. At strong gauge coupling, chiral symmetry is spontaneously broken and the monopole condensate is large and near its saturation value of unity. Both the chiral condensate and the monopole concentrations are hardly fluctuating at β in the vicinity of 0.90 since their respective susceptibilities are relatively tiny there. However, there is a clear jump in the monopole concentration to “zero” at $\beta \approx 0.956$ and the chiral condensate experiences a discontinuity here also, but it does not vanish. The chiral condensate will be discussed below. Here we concentrate on the monopole physics first although the chiral transition is the real focus and the original contribution of this work.

Conventional wisdom states that the transition at $\lambda = 1.4$ and $\beta \approx 0.956$ corresponds to confinement-deconfinement. On the strong coupling side of this point there is a monopole condensate which causes confinement [11] in the sense that all the physical states are neutral and the electric charge is a good quantum number. In such a phase one expects and finds chiral symmetry breaking. In Fig. 1 we show the monopole

TABLE I. Observables measured on a 16^4 lattice with four-Fermi coupling $\lambda = 1/G = 1.4$.

β	σ	χ_σ	M	χ_M	Trajectories
0.800	0.6556(10)	1.43(20)	0.99067(2)	0.451(2)	1500
0.900	0.6153(10)	1.61(23)	0.96809(5)	0.1787(4)	2550
0.950	0.5614(10)	2.05(40)	0.8890(2)	0.809(2)	2500
0.953125	0.5519(18)	6.11(50)	0.8708(2)	0.991(3)	3350
0.95625	0.4674(10)	3.21(52)	0.263(1)	27.6(3)	4350
0.9625	0.4416(15)	6.23(55)	0.0179(1)	16.52(4)	5100
0.975	0.4182(18)	2.49(47)	0.0423(6)	16.0(1)	1000
0.9875	0.4039(21)	3.35(50)	0.0661(5)	18.6(2)	1100
1.000	0.3822(10)	4.32(53)	0.0214(1)	9.00(1)	8200
1.050	0.3244(15)	4.52(37)	0.0001(1)	6.082(6)	2700
1.100	0.2798(10)	7.80(56)	0.0001(1)	5.352(3)	14150
1.150	0.2346(15)	11.2(1.0)	0.0001(1)	6.17(2)	6600
1.200	0.1856(15)	18.37(1.6)	0.0001(1)	4.751(2)	10900
1.225	0.1630(21)	25.58(2.4)	0.0001(1)	4.678(4)	7100
1.250	0.1394(18)	23.41(2.1)	0.0001(1)	4.601(3)	8400
1.2625	0.1281(27)	28.51(2.9)	0.0001(1)	4.568(4)	6000
1.275	0.1153(27)	41.67(4.6)	0.0001(1)	4.539(4)	5200
1.2875	0.0997(24)	37.03(3.7)	0.0001(1)	4.511(4)	4600
1.29375	0.0897(25)	40.0(4.3)	0.0001(1)	4.501(5)	5400
1.300	0.092(5)	50.0(6.5)	0.0001(1)	4.487(4)	5300
1.350	0.042(5)	35.7(4.1)	0.0001(1)	4.413(6)	4000
1.400	-0.021(5)	35.6(3.7)	0.0001(1)	4.356(6)	5000
1.500	-0.024(7)	29.5(5.1)	0.0001(1)	4.26(1)	2200
1.600	-0.005(5)	33.6(4.2)	0.0001(1)	4.194(9)	5850
1.700	-0.005(5)	31.5(3.7)	0.0001(1)	4.17(2)	2400

concentration as a function of β and suggest that there is a discontinuity in the graph.

Attempts to fit the concentration data with a power law that would be indicative of a steep but continuous transition failed badly. For example, a power law fit of the standard variety, $A(\beta_c - \beta)^{\beta_{mono}}$, to the points between $\beta=0.90$ and $\beta=0.95625$ had a χ^2 per degree of freedom in excess of 300 and an exponent $\beta_{mono} < 0.025$. The fit strongly suggests that

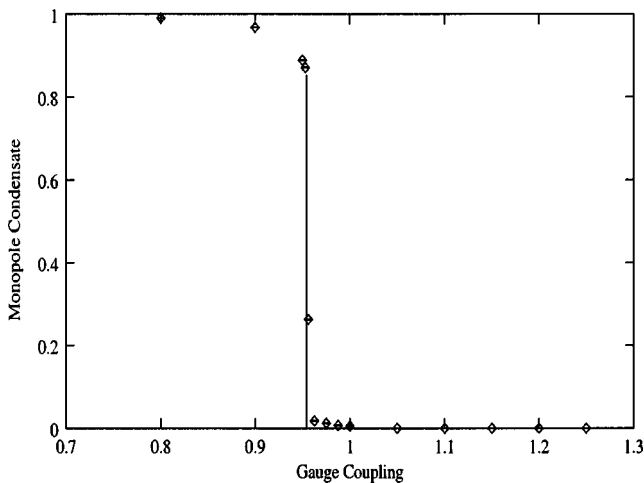


FIG. 1. Monopole concentration vs gauge coupling β at fixed four-Fermi coupling $\lambda = 1.4$, 16^4 lattice.

a step function discontinuity is preferred as shown in the figure.

Additional qualitative evidence for the first order character of the transition comes from the monopole susceptibility. We see in Table I that χ_M is highly spiked at the transition, jumping from 0.991(3) at $\beta=0.953125$ to 27.6(3) at $\beta = 0.95625$ and then falling to 16.52(4) on the weak coupling side of the transition at $\beta=0.9625$. This suggests that the real susceptibility is a delta function in the large volume thermodynamic limit. To really establish this claim, one would need a finite size study to monitor the size of the transition region and the height of the susceptibility curves as a function of volume.

Now consider the major focus of this paper, the chiral transition at fixed $\lambda = 1.4$. The raw data are shown in Table I and are plotted in Fig. 2

At strong coupling chiral symmetry is strongly broken and the chiral condensate is large and does not fluctuate severely. As in past studies, it proves convenient to monitor chiral symmetry breaking through the vacuum expectation value of the auxiliary field σ [4,12,1]. The quark-antiquark bilinear was also calculated in the simulation and is proportional to σ , in accordance with the theory's equations of motion [12].

The first interesting feature of this figure is the jump of the chiral condensate at $\beta=0.956$, at the same point where the monopole concentration fell to zero. The fact that Fig. 2

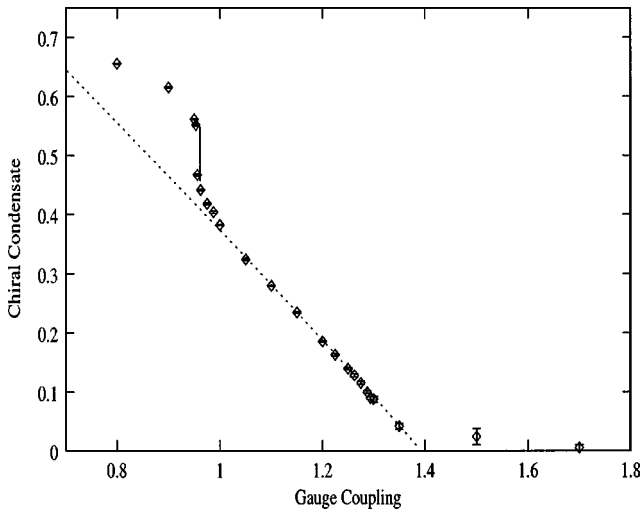


FIG. 2. Chiral condensate σ vs gauge coupling β at fixed four-Fermi coupling $\lambda=1.4$. 16^4 lattice. The dashed line is the power law fit discussed in the text.

has a jump at $\beta=0.956$ is further support for the first order character of the deconfinement transition there. It is also interesting that the chiral condensate does not vanish on the weak coupling side of the deconfinement transition. Apparently, the strong interactions in the theory are sufficient to cause chiral symmetry breaking without confinement. We expect that the theory has a rich spectrum of bound states on the weak coupling side of the transition at $\beta=0.956$ and $\lambda=1.4$, in accord with the physical picture of chiral symmetry breaking in Ref. [13]. It might be informative to do spectrum calculations in light of this result. It is very significant and nontrivial that the chiral condensate does not vanish on the weak coupling side of the deconfinement transition at $\beta=0.956$ and $\lambda=1.40$. Chiral symmetry breaking observed here is not due to the four-Fermi interaction alone. We know from Ref. [4] that a much stronger four-Fermi interaction, $G \approx 2$, is needed to break chiral symmetry in the absence of gauge interactions. In addition, simulations of compact QED with four species of staggered fermions but no four-Fermi interaction [9] produced chiral condensates on the weak coupling side of the transition which were consistent with zero. Physical mechanisms that could be causing substantial chiral symmetry breaking in this region of the phase diagram will be discussed in the last section of this paper.

Returning to Fig. 2, we see that the chiral condensate falls essentially linearly in the gauge coupling $\beta=1/e^2$ until a chiral symmetry restoration transition is found in the vicinity of $\beta_c=1.393(1)$ and $\lambda=1.4$. As recorded in Table I, the Monte Carlo statistics in this region of the phase diagram were quite considerable on this 16^4 lattice. Nonetheless, as the critical point was approached, there were the usual troubles with critical slowing down and tunnelling that hamper the predictive power of these results. Critical slowing down causes the rising statistical error bars recorded in Table I as β approaches the transition. Tunnelling between Z_2 vacua also became significant for $\beta \geq 1.29$ and limited our ability to simulate too close to the critical point. Notice that the four-Fermi term in the extended action is chosen to have

a Z_2 chiral symmetry which is spontaneously broken when σ develops a vacuum expectation value. This symmetry was chosen for the four-Fermi term because it is particularly easy to simulate and extract observables. In particular, as long as the theory resides in a particular chiral vacuum, σ and $\bar{\psi}\psi$ can be measured directly, without the need for inserting a small bare fermion mass into the theory to pick out a unique vacuum state. This is a great advantage because a bare fermion mass breaks chiral symmetry explicitly and leads to “rounding” of the transition which makes quantitative studies of the transition and its universality class very difficult.

The tunnelling between the two Z_2 vacua, $\sigma \rightarrow -\sigma$, limits our approach to the critical point and appears to be the most damaging finite size effect we must deal with. Simulations are planned on larger lattices to lessen it. Of course, the simulations of this study on a 16^4 lattice with high statistics represent a serious first step in this program.

Examining Table I, we note that the error bars in the σ and χ data are particularly large for β between 1.30 and 1.40, reflecting the occasional, every thousand or so time intervals, tunnelling between Z_2 vacua. The data for these points will not be used in the fits quoted here. Unfortunately, omitting these data means that this simulation may not be sensitive to the real critical behavior of the model. For example, the span of couplings from $\beta=1.1$ to 1.275 used in the fits here might extend only between 1.30 and 1.40. It might be that we need data in this region to confirm that this model has the “expected” logarithmically trivial scaling laws, like the noncompact model with four-Fermi terms [1]. This possibility and other issues of “conventional wisdom” will be reviewed in the section on conclusions below. At this point we will just do what we can do and plot and fit the order parameter and susceptibility data where the finite size effects appear to be under control.

In Fig. 2 we show the data on the chiral condensate fitted with a simple power law, $\sigma=A(\beta_c-\beta)^{\beta_{mag}}$. The fit takes the data at β ranging from 1.1 through 1.275 and finds $\beta_{mag}=0.96(9)$ and $\beta_c=1.393(1)$. The confidence level of the fit is excellent, 89%, corresponding to a χ^2 per degree of freedom of 1.12/4. The central value for the magnetic critical exponent β_{mag} is unchanged by taking wider ranges of couplings and even approaching the apparent critical point at $\beta_c=1.393(1)$ more closely, but the confidence levels deteriorate. We had expected a logarithmically improved mean field fit here with the magnetic critical exponent near 1/2, as was found in the noncompact QED case in [1], but there is no sign of that behavior. A value of $\beta_{mag}=0.96(9)$ suggests a nontrivial interacting theory, and is very perplexing, as will be discussed in the concluding section below.

We also accumulated the fluctuations in the order parameter, the susceptibility χ , as shown in Fig. 3. The values of χ in the immediate vicinity of $\beta_c=1.393(1)$ are certainly not reliable because of finite size effects and tunnelling. However, the trend for the susceptibility to grow rapidly from $\beta=1.00$ to 1.275 is clear and finite size effects appear to be under control on the 16^4 lattice over this limited range of couplings. Therefore, we attempted power law fits to the data

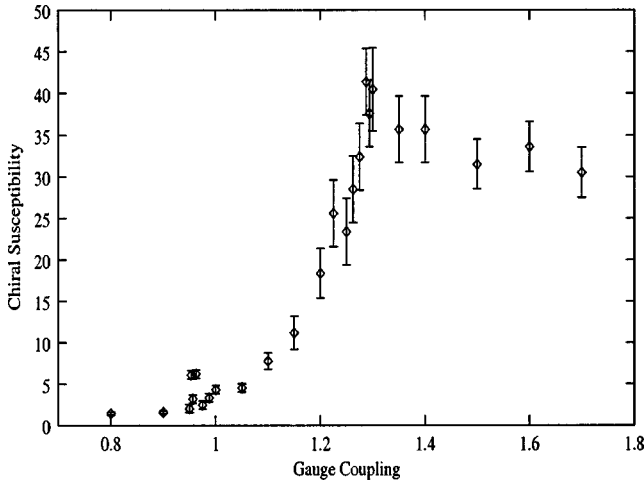


FIG. 3. Chiral susceptibility χ vs gauge coupling β at fixed four-Fermi coupling $\lambda = 1.4$. 16^4 lattice.

and in the next figure, Fig. 4, we show the reciprocal of the susceptibility, χ^{-1} , fitted to the data over the range $\beta = 1.05$ through 1.30 , $\chi^{-1} = B(\beta_c - \beta)^\gamma$.

The fit is quite good, having a confidence level of 48%, χ^2 per degree of freedom (DOF) = 7.5/8. The critical index for the susceptibility is predicted to be $\gamma = 3.1(3)$ and the critical coupling is again found to be $\beta_c = 1.393(1)$. It is interesting that γ is far from its means field value of unity, although our reservations about this data are the same as our reservations for the order parameter data and their fit.

The possible physical significance of this result will be discussed in the section on conclusions below. Since susceptibilities typically are more sensitive to finite size effects than the order parameter, it would be particularly informative to repeat this simulation on a larger lattice and attempt to track the height of the susceptibility peak as a function of lattice size to determine γ/ν , where ν is the correlation length exponent, by finite size scaling methods.

V. 16^4 SIMULATIONS AT FIXED $\beta = 1.00$

We also investigated the character of the monopole condensation transition at a different point in the model's two-parameter coupling space by setting the gauge coupling to a weaker value, $\beta = 1.00$, and varying λ . We started the simulations at strong four-Fermi couplings, large G or small $\lambda = 1/G$, as given in Table II. For example, at $\lambda = 0.20$, the monopole concentration M is large, $M = 0.8480(3)$, and its associated susceptibility is small, $\chi_M = 1.24(1)$. In addition, the chiral order parameter σ is large, $2.909(1)$, at this parameter set and its susceptibility is modest, $5.35(5)$, indicating that the fermions are irrelevant to the long distance dynamics in the model. Throughout the entire λ range, from 0.20 through 0.90 presented in Table II, the fermions remain very massive. However, the monopole concentration experiences a deconfinement transition near $\lambda = 0.5625$. As shown in Fig. 5, the transition appears to be a discontinuity, indicating a first order transition. In fact, power law fits to the monopole concentration data near $\lambda = 0.5625$ of the form $C(\lambda_c - \lambda)^{\beta_{mono}}$ produced very small indices, $\beta_{mono} < 0.10$, and very poor confidence levels, $\chi^2/\text{DOF} > 1000$. This result strongly suggests that this transition is actually first order, with a step discontinuity, in agreement with the results found at weaker four-Fermi coupling, $\lambda = 1.4$ and $\beta \approx 0.956$, discussed in the previous section.

Note from Table II that huge statistics, more than 10 000 Monte Carlo time units, were accumulated near the transition to deal with the slow relaxation of the gauge fields using our local, small change algorithm.

VI. CONCLUSIONS

When we began this study we believed that the monopole transitions would be very abrupt, perhaps first order, and that the chiral transitions would be described by mean field theory, decorated by the logarithms of triviality, as found in the noncompact theory [1]. Our expectations for the monopole transition held true, although it took orders of magni-

TABLE II. Observables measured on a 16^4 lattice with gauge coupling $\beta = 1.0$.

β	σ	χ_σ	M	χ_M	Trajectories
0.200	2.909(2)	5.35(75)	0.8480(3)	1.24(1)	650
0.300	2.2450(18)	3.61(50)	0.8341(4)	1.39(1)	550
0.400	1.8271(10)	3.75(51)	0.7967(4)	1.857(7)	2200
0.500	1.5370(6)	3.35(35)	0.7378(4)	2.762(8)	12200
0.525	1.4760(7)	2.76(35)	0.6824(3)	3.75(1)	9650
0.550	1.4180(5)	2.64(34)	0.6162(3)	5.19(1)	10200
0.5625	1.3839(7)	3.15(50)	0.0350(3)	31.6(2)	6650
0.575	1.3592(6)	3.17(45)	0.0532(5)	32.8(1)	11200
0.5875	1.3327(6)	2.75(45)	0.0351(3)	30.3(1)	8700
0.59375	1.3180(5)	2.83(36)	0.0372(6)	27.5(2)	10600
0.600	1.3086(6)	3.58(35)	0.085(1)	22.2(2)	6100
0.700	1.1233(8)	2.34(55)	0.0198(2)	18.54(7)	1700
0.800	0.9784(8)	3.85(45)	0.0150(2)	15.33(7)	3800
0.900	0.8485(7)	3.05(48)	0.0149(2)	13.37(6)	2600

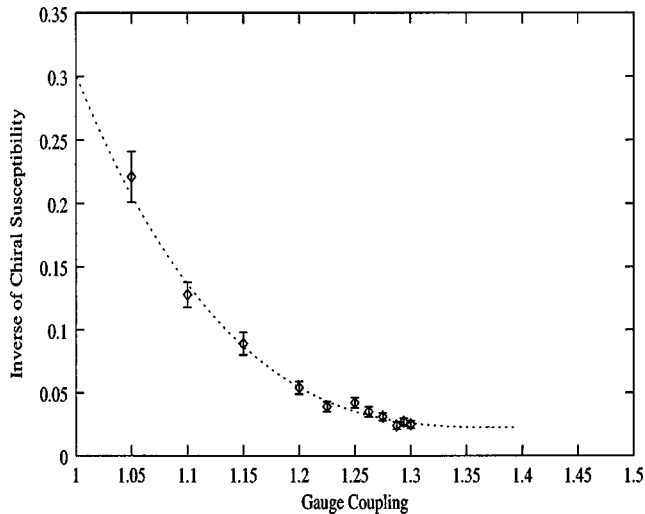


FIG. 4. Reciprocal of the chiral susceptibility χ vs gauge coupling β at fixed four-Fermi coupling $\lambda = 1.4$. 16^4 lattice. The dashed line is the power law fit discussed in the text.

tude more computer time to come to a decisive conclusion. We believed that the chiral transition would be described by logarithmically improved mean field theory, as found for the noncompact theory, because the monopole concentration would be vanishingly small in the vicinity of the chiral transition, the compact form of the action would become irrelevant, and the gauge field dynamics would reduce to photon exchanges, just as in the noncompact model. Only if we could somehow tune the two couplings to that region of the phase diagram where the first order confinement-deconfinement transition met the continuous chiral transition did we believe there was any possibility of interesting physics.

So we are left with a puzzling result: The chiral transition appears to have critical indices far from mean field theory. Just to illustrate and emphasize this point, assume hyperscaling and replace our numerical measurements of the critical indices with the integer predictions $\beta_{mag}=1$ and $\gamma=3$ they are consistent with. Then the remaining critical indices would be $\nu=5/4$, $\eta=-2/5$, $\delta=11/4$, and $\alpha=-3$. Are such large deviations from mean field behavior possible? When this model was studied in the limit of vanishing gauge couplings, the chiral transition was shown, both analytically [14], and numerically [4], to be described by logarithmically improved mean field theory. The algorithm used here but for vanishing gauge coupling gave results in fine agreement with $1/N$ analyses. Even the exponents of the logarithms of triviality were compatible with theoretical expectations, even though logarithms that decorate power law scaling laws are notoriously difficult to pin down. The extreme stability and accuracy of the algorithm that uses the fermion dynamical mass to regulate it and guide it was cited as a reason for this numerical success. If the “results” of this paper are correct, then we must conclude that the critical indices of the chiral transition vary as functions of λ and β and the four-Fermi interaction is not irrelevant along the line of chiral transitions. Conventional wisdom, based on perturbation theory, would say that fermion vacuum polarization would always

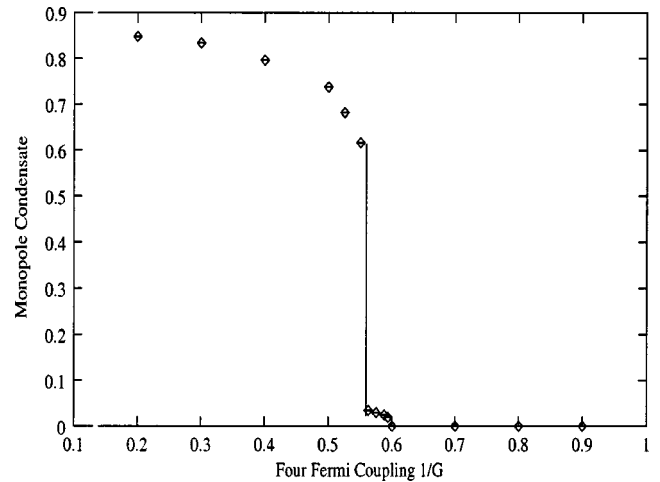


FIG. 5. Monopole concentration vs four-Fermi coupling $\lambda = 1/G$ at fixed gauge coupling $\beta=1.00$. 16^4 lattice.

screen the gauge couplings to zero leaving behind a Nambu–Jona-Lasinio model that has no interactions in a relativistic continuum limit.

What could the explanation of the simulation results of this study be? The obvious one is just that these results are wrong, in the sense that they are not indicative of the true continuum limit of the theory. Perhaps if we could simulate on larger lattices, closer to the critical point, we would find that the true critical behavior is, indeed, logarithmically improved mean field theory as was found by exactly the same methods for the noncompact gauged Nambu–Jona-Lasinio theory [1]. Perhaps the region from $\beta \approx 1.00$ to 1.3 at fixed $\lambda = 1.4$ is outside the real scaling region and is strongly affected by irrelevant but large nonlinearities in the Wilson action for the compact gauge fields. It may be that much larger lattices and much larger correlation lengths are needed to find the true continuum behavior in this model due to unusually large corrections to scaling for this particular action.

We believe that these issues should be decided and our only tool that avoids uncontrollable approximations is numerical simulations. This is a pity. Even numerical methods are sorely taxed by this problem. Nonetheless, simulations on larger lattices, closer to the continuum limit, are planned. Now that we know the interesting regions of the phase diagram, we can focus in and, hopefully, get to the heart of the matter more efficiently than in this exploratory, but time consuming study.

Early analytic studies of the gauged Nambu–Jona-Lasinio model within a framework which included only ladder Feynman diagrams [15] and which explicitly excluded fermion vacuum polarization predicted a line of nontrivial chiral transitions in the two-coupling phase diagram. It cannot be stressed too strongly, however, that this calculation was meant as a model of technicolor interactions and was not a solution of a field theory. It did not even include those effects, fermion loops and vacuum polarization, that are expected to render the theory trivial. However, other approximate approaches to this model which may account for screening to some degree have found a nontrivial line of

chiral transitions [16]. The reliability of this newer approximate approach is doubtful, however, because it predicts, contrary to the simulation results of [1], that even the noncompact gauged Nambu–Jona-Lasinio model is nontrivial. The work reported here and in Ref. [1] indicates that the noncompact model is logarithmically trivial while the compact model may not be, contrary to [16].

Let us end this discussion with some speculations which could guide the next generation of simulations planned for this model. Suppose that the preliminary results presented here are basically correct. What sort of physical excitations and interactions could support these results and how could they be discovered in the course of a numerical study? The middle region of Fig. 2 extending from the confinement-deconfinement transition at $\beta=0.956$ to the chiral transition at $\beta=1.393$ needs clarification. In this region $\langle \bar{\psi}\psi \rangle$ is non-zero while the monopole concentration M vanishes. Conventional wisdom suggests that the confinement-deconfinement transition is a four-dimensional generalization of the Kosterlitz-Thouless transition [17] which describes the two-dimensional planar spin model. In the two-dimensional Kosterlitz-Thouless transition a state of vortex-antivortex “molecules” ionizes and forms a plasma of vortices and antivortices. In four-dimensional pure compact QED, the confinement-deconfinement transition should be driven by the ionization of strands of bound monopole-antimonopole loops into a plasma of unbound individual loops of monopoles and loops of antimonopoles that causes confinement through the formation of electric flux tubes [11].

If the region of the phase diagram shown in Fig. 2 really consists of bound monopole-antimonopole strands, then we have a hint how the short distance properties of this theory can be qualitatively different from noncompact QED. In particular, the monopole-antimonopole pairs, which can exist in the compact model but not in the noncompact one, provide a medium that antiscreens electric charge. In classical electrodynamics, such an environment raises the fundamental electric charge of an impurity e^2 to ϵe^2 , where ϵ is the permit-

tivity of the vacuum. For a dilute background of monopole-antimonopole dipoles, each having a mean magnetic dipole moment of μ , one finds that $\epsilon=1+c\rho\mu^2$, where c is a positive constant and ρ is the density of the magnetic dipoles. The bound monopole-antimonopole strands could be a candidate mechanism for cancelling the screening provided by the light fermion-antifermion pairs.

Other ideas concerning screening and antiscreening in compact gauge theories, such as “collapse of the wave function” and “catalysis of symmetry breaking” [18], ideas inspired by monopole-induced proton decay [19], should be considered in this framework again and might be ingredients in a successful quantitative implementation of the monopole-antimonopole scenario suggested here.

Apparently there is still much to learn in this difficult subject of strongly coupled gauge theories. Luckily, advances in computer simulation power make many of these issues testable in the next round of investigations. In particular, we plan measurements of the vacuum permittivity ϵ , the renormalized electric charge and the renormalized four-Fermi coupling, the monopole-antimonopole spatial distribution in the vicinity of an external charge, etc. Measurements of the chiral condensate will be supplemented with measurements of the eigenvalue spectrum of the Dirac operator and the reliability of the algorithm with the four-Fermi term will be studied in greater detail.

Perhaps some analytical progress can also be made. The Dirac quantization condition, electric-magnetic duality transformations, and other ingredients of quantum electromagnetodynamics [20] might be considered in this framework of chiral symmetry breaking.

ACKNOWLEDGMENTS

J.B.K. was partially supported by NSF under grant NSF-PHY01-02409 and C.G.S. was supported by a Leverhulme Trust grant. The simulations were done at NPACI and NERSC. Special thanks go to NERSC for their long-term support.

-
- [1] S. Kim, J. B. Kogut, and M.-P. Lombardo, Phys. Lett. B **502**, 345 (2001); Phys. Rev. D **65**, 054015 (2002).
 - [2] S. Duane and J. B. Kogut, Phys. Rev. Lett. **55**, 2774 (1985); S. Gottlieb, W. Liu, D. Toussaint, R. L. Renken, and R. L. Sugar, Phys. Rev. D **35**, 2531 (1987).
 - [3] A. Kocić, J. B. Kogut, and S. Hands, Nucl. Phys. **B357**, 467 (1991).
 - [4] S. Kim, A. Kocić, and J. B. Kogut, Nucl. Phys. **B429**, 407 (1994).
 - [5] G. Arnold, B. Bunk, Th. Lippert, and K. Schilling, hep-lat/0210010.
 - [6] B. Rosenstein, B. Warr, and S. Park, Phys. Rep. **205**, 497 (1991).
 - [7] K. G. Wilson, Phys. Rev. D **10**, 2445 (1974).
 - [8] Y. Cohen, S. Elitzur, and E. Rabinovici, Nucl. Phys. **B220**, 102 (1983).
 - [9] E. Dagotto and J. B. Kogut, Phys. Rev. Lett. **59**, 617 (1987).
 - [10] S. Hands and R. Wensley, Phys. Rev. Lett. **63**, 2169 (1989).
 - [11] R. Myerson, T. Banks, and J. B. Kogut, Nucl. Phys. **B129**, 493 (1977).
 - [12] J. B. Kogut, J.-F. Lagae, and D. K. Sinclair, Phys. Rev. D **58**, 034504 (1998); J. B. Kogut and D. K. Sinclair, *ibid.* **64**, 034508 (2001).
 - [13] A. Casher, Phys. Lett. **83B**, 395 (1979).
 - [14] A. Kocić and J. Kogut, Nucl. Phys. **B422**, 593 (1994).
 - [15] C. N. Leung, S. T. Love, and W. A. Bardeen, Nucl. Phys. **B327**, 649 (1986).
 - [16] V. Azcoiti, G. Di Carlo, A. Galante, A. F. Grillo, and V. Laliena, Phys. Lett. B **416**, 409 (1998).
 - [17] J. M. Kosterlitz and D. J. Thouless, J. Phys. C **6**, 118 (1973).
 - [18] E. Dagotto, A. Kocić, and J. B. Kogut, Phys. Rev. Lett. **62**, 1001 (1989).
 - [19] V. A. Rubakov, Nucl. Phys. **B203**, 311 (1982).
 - [20] M. Blagojevic and P. Senjanovic, Phys. Rep. **157**, 233 (1988).